Article

Studies of Organically Functionalized Mesoporous Silicas Using Heteronuclear Solid-State Correlation NMR Spectroscopy under Fast Magic Angle Spinning

Julien Trebosc, Jerzy W. Wiench, Seong Huh, Victor S.-Y. Lin, and Marek Pruski

J. Am. Chem. Soc., **2005**, 127 (20), 7587-7593• DOI: 10.1021/ja0509127 • Publication Date (Web): 30 April 2005

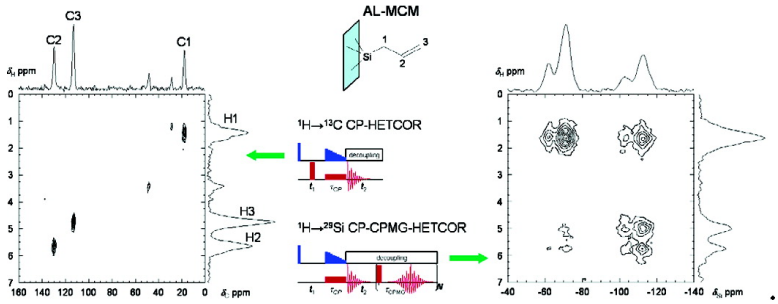

More About This Article

Additional resources and features associated with this article are available within the HTML version:

- Supporting Information
- Links to the 16 articles that cite this article, as of the time of this article download
- Access to high resolution figures
- Links to articles and content related to this article
- Copyright permission to reproduce figures and/or text from this article

View the Full Text HTML

J|A|C|S
ARTICLES
Published on Web 04/30/2005

Studies of Organically Functionalized Mesoporous Silicas Using Heteronuclear Solid-State Correlation NMR Spectroscopy under Fast Magic Angle Spinning

Julien Trebosc,[†] Jerzy W. Wiench,[†] Seong Huh,[†,‡] Victor S.-Y. Lin,[†,‡] and Marek Pruski*[,†]

Contribution from the Ames Laboratory and Department of Chemistry, Iowa State University, Ames, Iowa 50011-3020

Received February 23, 2005; E-mail: mpruski@iastate.edu

Abstract: Highly resolved solid-state HETCOR NMR spectra between protons and low gamma nuclei (^{13}C and ^{29}Si) can be suitably obtained on surfaces using a "brute force" ^{1}H−^{1}H decoupling by MAS at rates ≥40 kHz. Despite a small rotor volume (<10 μL), a ^{1}H−^{13}C HETCOR spectrum of allyl groups (AL, −CH_2−CH=CH_2) covalently anchored to the surface of MCM-41 silica was acquired without using isotope enrichment. The advantages of using fast MAS in such studies include easy setup, robustness, and the opportunity of using low RF power for decoupling. In the case of the ^{1}H−^{29}Si HETCOR experiment, the sensitivity can be dramatically increased, in some samples by more than 1 order of magnitude, through implementing into the pulse sequence a Carr−Purcell−Meiboom−Gill train of π pulses at the ^{29}Si spin frequency. The use of low-power heteronuclear decoupling is essential in the ^{1}H−^{29}Si CPMG-HETCOR experiment, due to unusually long acquisition periods. These methods provided detailed structural characterization of the surface of AL-MCM mesoporous silica.

1. Introduction

Detailed information about the structure, topology, and dynamics of complex molecular systems may be best provided by multidimensional homo- and heteronuclear correlation (HETCOR) NMR, which offers improved resolution by separating the resonances in two or more dimensions, and reveals through-space or through-bond connectivities between spins. In solids, high spectral resolution is obtained by using various combinations of radio frequency (RF) pulse sequences with mechanical rotation of the sample, typically under the condition of magic angle spinning (MAS).[1] The major experimental challenge associated with application of two-dimensional (2D) ^{1}H−X (X = ^{29}Si, ^{13}C, ^{31}P, ^{15}N, ...) correlation experiments under MAS involves suppressing ^{1}H−^{1}H homonuclear dipolar interactions during the evolution period, such that the isotropic chemical shift and resonance offsets dominate the behavior of ^{1}H magnetization in the indirect dimension. Early approaches[2−4] utilized multipulse decoupling schemes in a quasi-static approximation, which required the use of low sample rotation rates.[5] More recent methods used symmetry-based sequences[6,7] or Lee−Goldburg (LG) schemes,[8−10] which proved effective in the ^{1}H−^{13}C HETCOR experiments performed under fast MAS.[9,10] Maintaining good efficiency and selectivity of through-space ^{1}H−X polarization transfer under fast MAS poses another important challenge. While standard cross polarization (CP) is most commonly used, other techniques, such as MREV-8,[3] windowless isotropic mixing (WIM),[4] or LG irradiation, were extensively studied for efficiency and selectivity reasons.[11] During such transfers, the ^{1}H nuclei can be isolated from each other, which eliminates "artificial" cross-peaks resulting from ^{1}H−^{1}H spin diffusion, allows for spectral editing, and provides opportunities for measuring internuclear distances between ^{1}H and X. Applications of these methods encompass a wide variety of crystalline and amorphous materials, including polymers and other organic,[3,4,12] organic/inorganic nanocomposites,[13−15] and biochemical compounds.[2,9−11,16] ^{1}H−^{29}Si and ^{1}H−^{13}C

[†] Ames Laboratory.
[‡] Department of Chemistry.

(1) Haeberlen, U. *High-Resolution NMR in Solids: Selective Averaging*; Academic Press: New York, 1976.
(2) Caravatti, P.; Braunschweiler, L.; Ernst, R. R. *Chem. Phys. Lett.* **1983**, *100*, 305−310.
(3) Roberts, J. E.; Vega, S.; Griffin, R. G. *J. Am. Chem. Soc.* **1984**, *106*, 2506−2512.
(4) Burum, D. P.; Bielecki, A. *J. Magn. Reson.* **1991**, *94*, 645−652.
(5) Gerstein, B. C.; Pembleton, R. G.; Wilson, R. C.; Ryan, L. M. *J. Chem. Phys.* **1977**, *66*, 361−362.
(6) Hafner, S.; Spiess, H. W. *J. Magn. Reson. A* **1996**, *121*, 160−166.
(7) Madhu, P. K.; Zhao, X.; Levitt, M. H. *Chem. Phys. Lett.* **2001**, *346*, 142−148.
(8) Bielecki, A.; Kolbert, A. C.; de Groot, H. J. M.; Griffin, R. G.; Levitt, M. H. *Adv. Magn. Reson.* **1990**, *14*, 111−124.
(9) Vinogradov, E.; Madhu, P. K.; Vega, S. *Chem. Phys. Lett.* **2002**, *354*, 193−202.
(10) van Rossum, B. J.; Förster, H.; de Groot, H. J. M. *J. Magn. Reson.* **1997**, *124*, 516−519.
(11) Ladizhansky, V.; Vega, S. *J. Chem. Phys.* **2000**, *112*, 7158−7168.
(12) Bronnimann, C. E.; Ridenour, C. F.; Kinney, D. R.; Maciel, G. E. *J. Magn. Reson.* **1992**, *97*, 522−534.
(13) Hou, S. S.; Beyer, F. L.; Schmidt-Rohr, K. *Solid State Nucl. Magn. Reson.* **2002**, *22*, 110−127.
(14) Melosh, N. A.; Lipic, P.; Bates, F. S.; Wudl, F.; Stucky, G. D.; Fredrickson, G. H.; Chmelka, B. F. *Macromolecules* **1999**, *32*, 4332−4342.
(15) Brus, J.; Spirkova, M.; Hlavata, D.; Strachota, A. *Macromolecules* **2004**, *37*, 1346−1357.
(16) Ramamoorthy, A.; Wu, C. H.; Opella, S. J. *J. Magn. Reson.* **1999**, *140*, 131−140.

HETCOR NMR was also used to study the surface and interfacial species on zeolites,[17] silica,[18−21] and mesoporous aluminosilicates.[22]

The pursuit of highest sample rotation rates resulted in the construction of probes capable of MAS frequency (ν_R) of more than 50 kHz,[23,24] which allows for a "brute force" approach of very fast spinning to be increasingly used for ^{1}H−^{1}H decoupling, especially in samples with moderate or weak ^{1}H−^{1}H interactions. First examples of 2D applications include the ^{1}H−^{13}C INEPT spectra of uncalcined mesoporous silicas taken using $\nu_R = 35$ kHz[25] and the ^{13}C−^{13}C DREAM experiments with peptides and proteins performed at $\nu_R = 60$ kHz.[24] Herein, we demonstrate that the approach utilizing ultrafast MAS is very well suited for HETCOR NMR spectroscopy of the species chemically bound to surfaces. Specifically, we examine the structure and conformation of an allyl functional group (AL, −CH_2−CH═CH_2) covalently bonded to the surface of a MCM-41-type mesoporous silica material (AL-MCM) in the absence of templating molecules. We show that by employing ultrafast MAS, the ^{1}H−^{13}C HETCOR spectra of these surface species can be practically obtained without the isotopic enrichment using sample quantities not exceeding 10 mg. This approach compares favorably with the experiment performed with a much larger rotor, where the use of multipulse schemes is required for ^{1}H−^{1}H decoupling. Furthermore, we report that a dramatic improvement in sensitivity of ^{1}H−^{29}Si HETCOR spectra, performed under fast MAS, can be achieved by using the Carr−Purcell−Meiboom−Gill (CPMG)[26] train of π pulses during the acquisition period.

2. Experimental Section

Sample Synthesis. The AL-MCM material was synthesized via co-condensation by heating a mixture of cetyltrimethylammonium bromide surfactant ($CH_3(CH_2)_{15}N(CH_3)_3Br$), referred to as CTAB (2.0 g, 5.49 mmol), 2.0 M NaOH (aq) (7.0 mL, 14.0 mmol), and H_2O (480 g, 26.67 mol) at 80 °C for 30 min with a constant stirring (550 rpm).[27] To this clear solution were added sequentially and rapidly via injection tetraethoxysilane (9.34 g, 44.8 mmol) and allyltrimethoxysilane, denoted as ALTMS (1.03 g, 5.75 mmol). Following this procedure, a white precipitation was observed after 3 min of stirring at ca. 550 rpm. The as-made mesoporous material was obtained after an additional 2 h of heating at 80 °C, followed by hot filtration, washing with water and methanol, and drying under vacuum. An acid extraction was performed in a methanol (100 mL) mixture of concentrated hydrochloric acid (1.0 mL) and as-made AL-MCM material (1.0 g) at 60 °C for 6 h. The silica was then filtered, washed with water and methanol, and dried under vacuum for 3 h at 90 °C. The resulting material had the BET surface area of 1080 m^2/g and the average pore diameter of 2 nm. It was then packed in the MAS rotor in as-synthesized state (sample **A**). Another sample, labeled **B**, was prepared by dehydrating sample **A** at 100 °C under 10^{-5} atm and saturating it with deuterated water prior to the NMR measurements.

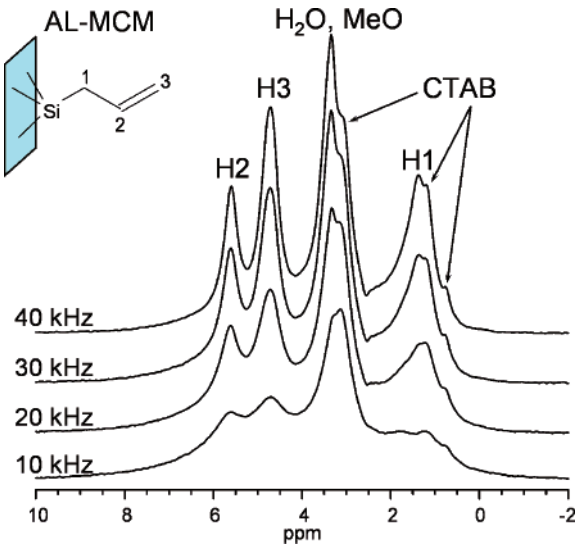

Figure 1. ^{1}H MAS NMR spectra of sample **A** taken with $\nu_R = 10$, 20, 30, and 40 kHz.

Solid-State NMR. Solid-state NMR experiments were performed at 9.4 T on a Chemagnetics Infinity spectrometer equipped with 5 and 1.8 mm (A. Samoson[23,28,29]) double-tuned probes capable of MAS at 10 and 50 kHz, respectively. Several implementations of the 2D NMR HETCOR experiment were tested, using the general schemes and experimental parameters described in sections 3.2 and 3.3.

Although the typical values of T_1 for ^{1}H nuclei measured in our samples ranged between 0.4 and 0.75 s, the acquisition delay was reduced to 1 or 1.5 s during the acquisition of HETCOR spectra. In experiments performed using fast MAS, the hypercomplex method was employed to discriminate the sine and cosine parts in the F_1 domain of 2D spectra. The 2D measurements with FSLG irradiation during the t_1 interval employed the so-called time-proportional phase increments (TPPI) approach to achieve sign discrimination in F_1. The standard phase cycling methods were used to select the signals from the desired coherence pathways. All ^{1}H, ^{29}Si, and ^{13}C chemical shifts are reported using the δ scale and are referenced to tetramethylsilane (TMS) at 0 ppm.

3. Results and Discussion

3.1. ^{1}H MAS NMR. Figure 1 shows the improvement in resolution observed in the ^{1}H NMR spectra of the as-synthesized AL-MCM (sample **A**) taken with increasing MAS frequency, ν_R. A similar effect was recently achieved in nonfunctionalized MCM-41 silicas.[30] The static spectrum of sample **A** (not shown) is a superposition of unresolved lines with widths of up to 10 kHz (fwhm), which are homogeneously broadened by the ^{1}H−^{1}H dipolar interactions. This line broadening is smaller than expected in strongly coupled ^{1}H spin systems, which implies that some degree of molecular mobility exists on the silica surface. The ^{1}H−^{1}H dipolar coupling was almost completely eliminated by sample spinning at 40 kHz. The residual line width

(17) Vega, A. J. *J. Am. Chem. Soc.* **1988**, *110*, 1049−1054.
(18) Fyfe, C. A.; Zhang, Y.; Aroca, P. *J. Am. Chem. Soc.* **1992**, *114*, 3252−3255.
(19) Fyfe, C. A.; Aroca, P. P.; Zhang, Y. *Bull. Magn. Reson.* **1993**, *15*, 195−198.
(20) Chabanas, M.; Baudouin, A.; Coperet, C.; Basset, J.-M.; Lukens, W.; Lesage, A.; Hediger, S.; Emsley, L. *J. Am. Chem. Soc.* **2003**, *125*, 492−504.
(21) Rataboul, F.; Baudouin, A.; Thieuleux, C.; Veyre, L.; Coperet, C.; Thivolle-Cazat, J.; Basset, J.-M.; Lesage, A.; Emsley, L. *J. Am. Chem. Soc.* **2004**, *126*, 12541−12550.
(22) Janicke, M. T.; Landry, C. C.; Christiansen, S. C.; Kumar, D.; Stucky, G. D.; Chmelka, B. F. *J. Am. Chem. Soc.* **1998**, *120*, 6940−6951.
(23) Samoson, A. In *Encyclopedia of Nuclear Magnetic Resonance*; Grant, D. M., Harris, R. K., Eds.; John Wiley & Sons: Chichester, U.K., 2002; Vol. 9, pp 59−64.
(24) Ernst, M.; Meier, M. A.; Tuherm, T.; Samoson, A.; Meier, B. H. *J. Am. Chem. Soc.* **2004**, *126*, 4764−4765.
(25) Alonso, B.; Massiot, D. *J. Magn. Reson.* **2003**, *163*, 347−352.
(26) Meiboom, S.; Gill, D. *Rev. Sci. Instrum.* **1958**, *29*, 688−691.
(27) Huh, S.; Wiench, J. W.; Yoo, J.-C.; Pruski, M.; Lin, V. S.-Y. *Chem. Mater.* **2003**, *15*, 4247−4256.
(28) Samoson, A.; Tuherm, T.; Past, J. *Chem. Phys. Lett.* **2002**, *365*, 292−299.
(29) Samoson, A.; Tuherm, T.; Past, J.; Reinhold, A.; Anupõld, T.; Heinmaa, I. *Top. Curr. Chem.* **2004**, *246*, 15−31.
(30) Trebosc, J.; Wiench, J. W.; Huh, S.; Lin, V. S.-Y.; Pruski, M. *J. Am. Chem. Soc.* **2005**, *127*, 3057−3068.

under MAS is controlled by the exchange processes and inhomogeneous contribution due to the distribution of chemical shifts.[30]

We could not further improve upon this resolution in AL-MCM by combining MAS with multipulse ^{1}H−^{1}H decoupling schemes, such as FSLG, regardless of the spinning frequency used. Clearly, however, the complete line narrowing cannot be, at present, achieved by fast MAS alone in the case of very strongly coupled systems of ^{1}H spins. For example, a spectrum of glycine, which we acquired under $\nu_R = 40$ kHz, exhibited 3−3.5 ppm wide lines, with the methylene protons being completely unresolved. In agreement with the earlier reports,[9] these lines were easily resolvable with the aid of the FSLG-2 sequence, where the observed widths were 0.75−0.85 ppm, both under MAS at 10 and 40 kHz. An artifact associated with the fast MAS approach is the frictional heating of the sample. By using the chemical shift of ^{207}Pb in lead nitrite as a thermometer,[31] we have determined that the rotor temperature increased by 10−15 °C above the ambient under $\nu_R = 40$ kHz.

The interpretation of the MAS spectra of Figure 1 is straightforward. To denote the silicon sites, we use the standard notation, in which the sites connected to four other silicon atoms via siloxane linkages are denoted as Q^4, the (≡SiO−)$_3$**Si**(OH) and (≡SiO−)$_2$**Si**(OH)$_2$ sites are labeled Q^3 and Q^2, and the (≡SiO−)$_3$**Si**R and (≡SiO−)$_2$**Si**(OR′)R sites are labeled T^3 and T^2, respectively. On the basis of our previous study,[30] the resonances at 0.8, 1.2, and 3.1 ppm are assigned to −CH_3, −CH_2−, and −CH_2−N$(CH_3)_3$ protons in the residual CTAB molecules remaining in the pores after the acid extraction. These molecules were found to be located in mostly prone positions along the channel walls in the areas occupied by the Q^4 silicon sites.[30] The resonances at 1.4, 4.7, and 5.6 ppm represent CH_2 and CH groups in AL, as shown in Figure 1. The rapidly exchanging ≡Si−OH···$(H_2O)_n$ species consisting of weakly adsorbed water that is hydrogen bonded to the silanol groups are represented by a peak centered at 3.4 ppm. The ^{1}H MAS spectra of as-synthesized, nonfunctionalized samples were dominated by this resonance, which appeared between 3 and 5 ppm depending on the value of n.[30] This peak also includes a contribution from the methoxy groups associated with T^2 silicon sites. The isolated ≡Si−OH species cannot be identified as a separate resonance in the 1D spectrum, but contribute to the intensity observed in the range of 2−2.5 ppm.

3.2. ^{1}H−X HETCOR. The sequence shown in Figure 2a (scheme **1**) is similar to that proposed by van Rossum et al.,[10] wherein the homonuclear decoupling is achieved by FSLG-2, the polarization transfer via ramped amplitude Hartmann−Hahn CP sequence (RAMP−CP),[32] and heteronuclear decoupling is applied during the acquisition period. The initial pulse in the ^{1}H channel rotates the magnetization by 90° + 54.7° = 144.7°, whereas the flip angle of the pulse following the evolution period is 54.7°. The experiment was performed using a large-volume (140 μL), 5 mm rotor under $\nu_R = 10$ kHz. However, the sample volume had to be reduced to approximately 50 μL in order to prevent the inhomogeneity of the RF magnetic field from degrading the ^{1}H resolution. The windowless FSLG-2 decoupling was chosen during t_1 evolution because of the high scaling factor (0.58), short cycle duration, efficient low-power operation,

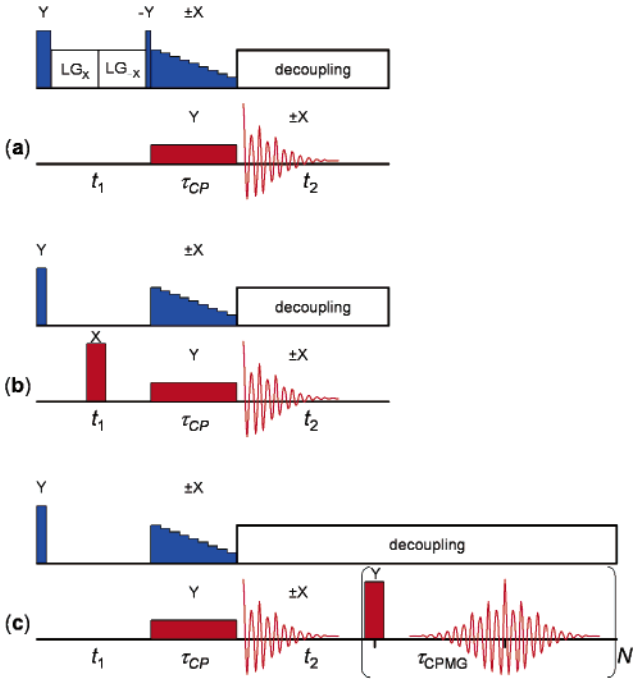

Figure 2. Pulse sequences for the 2D ^{1}H−X heteronuclear correlation spectra. (a) Scheme **1**, with FSLG-2 irradiation during t_1; (b) scheme **2**, with fast MAS; and (c) scheme **3**, with fast MAS and sensitivity enhancement by CPMG pulse sequence.

easy optimization (frequency offset and pulse length), and relatively high tolerance to pulse errors.[8,33] The interactions observed during t_1 are the scaled ^{1}H chemical shift, the resonance offset, and the scaled heteronuclear J coupling.

In the AL-MCM silica studied in this work, the RAMP-CP method proved to be efficient and easy to implement. The efficiency and selectivity of ^{1}H−X coherence transfer is, however, sample dependent. The suppression of ^{1}H−^{1}H dipolar coupling during mixing using suitable multipulse sequences in the ^{1}H and X channels may be advantageous in more rigid spin systems.[3,4] Efficient heteronuclear decoupling during the detection period could be obtained under high-power CW RF irradiation or via TPPM,[34] provided that the applied RF magnetic field strength exceeded ν_R by a factor of at least 3.

The pulse sequence shown in Figure 2b (scheme **2**) used $\nu_R = 40$ kHz without any additional RF irradiation in the ^{1}H channel during the evolution period. However, a single π pulse was introduced in the middle of the evolution period at the X spin frequency in order to refocus the J_{X-H} coupling, which would otherwise be fully operable under the conditions of this experiment. The π pulse can be similarly used with scheme **1** to refocus the (scaled) heteronuclear couplings. Again, the RAMP-CP method was used for the ^{1}H−X coherence transfer, and heteronuclear decoupling via TPPM was used for proton decoupling during the acquisition period. In this scheme, heteronuclear decoupling during t_2 could be suitably achieved by using CW irradiation at RF field strength corresponding to a precession frequency much smaller than ν_R.[35]

Given the number of intricate and often conflicting factors that influence the implementation of these two approaches, only

(31) Bielecki, A.; Burum, D. P. *J. Magn. Reson. A* **1995**, *116*, 215−220.
(32) Metz, G.; Wu, X.; Smith, S. O. *J. Magn. Reson. A* **1994**, *110*, 219−227.
(33) Bielecki, A.; Kolbert, A. C.; Levitt, M. H. *Chem. Phys. Lett.* **1989**, *155*, 341−346.
(34) Bennett, A. E.; Rienstra, C. M.; Auger, M.; Lakshmi, K. V.; Griffin, R. G. *J. Chem. Phys.* **1995**, *103*, 6951−6958.

the experiment could demonstrate which one provides a better overall performance. The spectrum of sample **A** taken using scheme **1** is shown in Figure 3a, whereas the corresponding result obtained using scheme **2** (without the π pulse in the X channel) is plotted in Figure 3b. The *J*-decoupled version of spectrum (b) is shown in Figure 3c. The most important experimental parameters are described in the figure caption, where ν_{RF}^{X} denotes the magnitude of the radio frequency field applied to X nuclei and τ_{CP} is the cross polarization time.

The 1D projections of these spectra along the ^{13}C dimension are very similar to the MAS NMR spectrum of AL-MCM material reported earlier,[27] which demonstrates that RAMP-CP under fast MAS yielded quite accurate spectra with both HETCOR schemes. As expected, the corresponding projections along the ^{1}H dimension do not show the resonances attributed to water and the hydroxyl groups. The observed cross-peaks correspond to C1−H1, C2−H2, and C3−H3 correlations in AL, as marked in spectrum (c). Also present are the less intense resonances representing the surface methoxy groups and the methylene groups in CTAB.

These assignments will be further corroborated by $^{1}H-^{29}Si$ HETCOR NMR (section 3.3) and reviewed in section 3.4. The discussion below is mainly confined to general experimental aspects of the applied methods. We first note that despite the relative sample volume being 5 times smaller (10 μL under fast MAS versus 50 μL in the FSLG experiment), scheme **2** provided spectra with very respectable overall signal-to-noise (S/N) ratio. Surprisingly good efficiency of the CP process and small diameter of the RF coil contributed to higher relative sensitivity of the fast MAS approach. In addition, the signal loss due to RF manipulations in the t_1 domain may have lessened the sensitivity of scheme **1**, despite the fact that only the central section of the rotor has been filled with the sample.

The best resolution in ^{1}H dimension is observed in spectrum (c), where the J_{CH} splittings have been refocused. The *J*-couplings are present in the scaled form in spectrum (a) and are evident in full strength of ~140 Hz in spectrum (b) of Figure 3. Note that the scalar (and dipolar) heteronuclear interactions cannot play any significant role in the ^{1}H MAS spectra of Figure 1 because the sample was not ^{13}C-enriched.

In scheme **1**, high resolution during t_1 can be also accomplished by applying a combination of $^{1}H-^{1}H$ and $^{1}H-X$ dipolar (and scalar) decoupling sequences, such as BLEW-12 and WALTZ,[2] BLEW-24 and BB-24,[4] or BLEW-48 and BB-48,[12] to protons and X nuclei, respectively. To minimize the adverse effects due to simultaneous application of MAS- and RF-driven time-dependent perturbations, the sequences must use short cycle times ($t_c < 1/\nu_R$) and be appropriately synchronized with a rotor.[6] The CW $^{1}H-X$ decoupling during t_1 can be used as well, provided that the RF power used does not interfere with homonuclear sequences.[3]

During the detection period, high-power ^{1}H decoupling is routinely used with scheme **1** to observe sharp ^{13}C resonances. Although in scheme **2** fast MAS alone provided reasonably good resolution, the line could be further narrowed, by a factor of approximately 2, under ^{1}H RF decoupling. However, high RF power was not required in this case, as decoupling schemes that use low power were shown to be equally effective at $\nu_R \geq$ 40 kHz.[35] Low-power XiX heteronuclear decoupling[36,37] was also shown to be very efficient in the $^{13}C-^{13}C$ DREAM

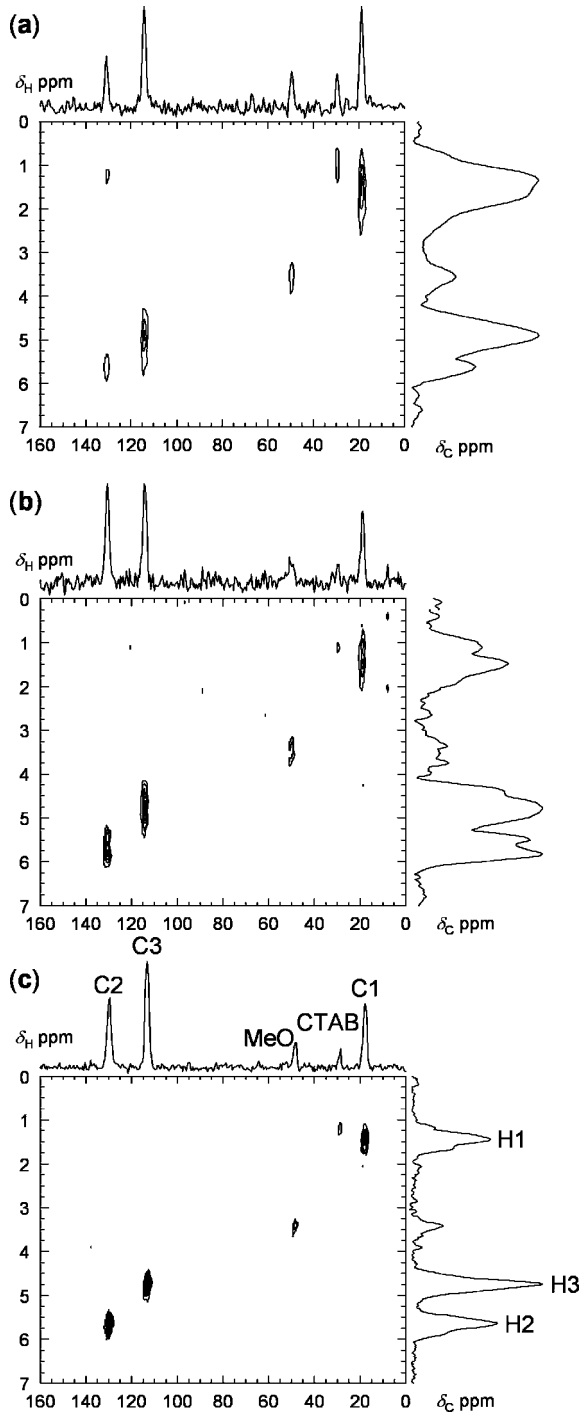

Figure 3. Two-dimensional heteronuclear $^{1}H-^{13}C$ correlation spectra of an allyl group ($-CH_2-CH=CH_2$) covalently bound to the pore walls of a MCM-41-type silica material (sample **A**) taken using schemes **1** (a) and **2** (b, c). Spectrum (a) was acquired using $\nu_R = 10$ kHz and $\nu_{RF}^{H} = 70$ kHz during FSLG-2 irradiation with a 4 kHz offset, $\nu_{RF}^{H} = 55-65$ kHz during RAMP-CP (11 steps), $\nu_{RF}^{C} = 50$ kHz during CP, $\tau_{CP} = 1.5$ ms, $\nu_{RF}^{H} = 90$ kHz during CW decoupling and the delay between scans of 1.5 s. Spectra (b, c) used $\nu_R = 40$ kHz and $\nu_{RF}^{H} = 100-140$ kHz during RAMP-CP (15 steps), $\nu_{RF}^{C} = 80$ kHz during CP, $\tau_{CP} = 1.5$ ms, $\nu_{RF}^{H} = 11$ kHz during CW (b) and TPPM (c) decoupling, and the delay between scans of 1 s. The 1D projections are shown in skyline mode. Although different t_1 increments and different numbers of scans were used, the total acquisition time was approximately 80 h in all experiments.

(35) Ernst, M.; Samoson, A.; Meier, B. H. *Chem. Phys. Lett.* **2001**, *348*, 293−302.

experiments performed using $\nu_R = 60$ kHz.[24] Indeed, we found that an RF magnetic field of 11 kHz was as useful as 130 kHz during ^{1}H CW decoupling. The same was observed for TPPM, which worked equally well in our experiments. The ability to use low-power decoupling can lessen the burden on the spectrometer and minimize the sample heating by the dissipated RF power. Besides, it enabled us to perform the CPMG-HETCOR experiment shown in section 3.3.

Additional advantages of scheme **2** in the study of these moderately coupled spin systems include the following: (i) good selectivity of the CP process, with little scrambling of ^{1}H−^{13}C correlations by ^{1}H−^{1}H spin diffusion, which is sufficiently attenuated by MAS alone; (ii) the decoupling schemes can still be used in addition to MAS, both during evolution and mixing periods; (iii) only the centerbands are observed in both dimensions; (iv) no scaling of interactions involving ^{1}H nuclei takes place; and (v) there is no destructive interference between MAS and multiple pulse sequences.[2,6] Finally, the experiment is very easy to set up.

3.3. ^{1}H−X CPMG-HETCOR. We have also achieved a remarkable enhancement of sensitivity in the ^{1}H−^{29}Si HETCOR spectra by applying a CPMG train of rotor-synchronized π pulses[26] during the detection of silicon magnetization. The CPMG sequence has been introduced at first to facilitate the measurements of T_2 relaxation via Hahn's spin−echo, as it refocuses the inhomogeneous line broadening and reduces the homonuclear dipolar broadening in solids.[38,39] In later studies, it has been adapted to enhance the sensitivity in various applications involving spin−$^1/_2$ and quadrupolar nuclei, including static,[40] MAS,[41,42] MQMAS,[43,44] and PHORMAT[45] experiments. The signal enhancement is a function of T_2 and the spacing τ_{CPMG} between the π pulses, which in turn depends on the signal decay following the single excitation pulse (often denoted as T_2^*). The spin−spin relaxation time T_2 describes here the decay of the echo train due to time-dependent interactions that are nonrefocusable by the π pulses under the conditions of the experiment. In favorable cases, sensitivity gains exceeding 1 order of magnitude have been achieved.[41,42,44]

The data obtained using the CPMG experiment can be processed by directly Fourier transforming the fully digitized echo train, acquired with proper blanking of the receiver during the pulses, which results in the so-called spikelet spectrum. Alternatively, the echoes can be co-added prior to Fourier transformation to produce a reconstructed spectrum. In the latter case, the resulting increase in sensitivity can be analytically expressed as

$$G(N) = \frac{1}{\sqrt{2N+1}} \frac{2x^{N+1} - x - 1}{x - 1} \qquad (1)$$

where N is the number of acquired echoes and $x = \exp(-\tau_{CPMG}/T_2)$. Equation 1 has been obtained by assuming that the CPMG spectrum includes contributions from all of the echoes and the initial free induction decay (FID), whose gain $G(0) = 1$. We note that the signal can be also acquired by "skimming" the top of the echoes which, however, results in a loss of chemical shift information. This strategy has been recently used for sensitivity enhancement in ^{1}H−^{29}Si HETCOR NMR of a clay mineral.[13]

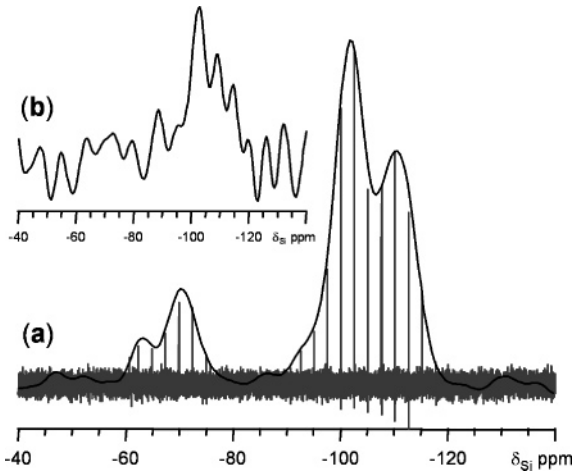

Figure 4. ^{1}H−^{29}Si CPMAS spectra of sample **A**. (a) Superposition of the "spikelet spectrum", resulting from Fourier transformation of 200 echoes (22 456 data points), with the spectrum reconstructed from the same dataset by co-adding the echoes as described in the text. (b) "Standard" MAS spectrum obtained by processing only the first FID. The echoes were acquired under the following experimental conditions: $\nu_R = 40$ kHz, $\tau_{CPMG} = 5.6$ ms, $\tau_{CP} = 10$ ms, $\nu_{RF}^H = 110-130$ kHz during RAMP-CP (16 steps), $\nu_{RF}^{Si} = 80$ kHz during CP and π pulses, $\nu_{RF}^H = 18$ kHz during TPPM decoupling, and a delay between scans of 2.6 s (including 1.1 s of data acquisition). The widths of the individual spikelets ranged from 0.3 Hz for Q^4 sites (at −115 ppm) to 0.5 Hz for T^2 sites (at −65 ppm).

The gain in S/N ratio is illustrated in Figure 4a,b, which includes the ^{1}H−^{29}Si CPMAS spectra of sample **A** obtained with and without the CPMG enhancement, respectively. The data were acquired using the experimental parameters listed in the figure caption. The reconstructed spectrum, represented by the solid line in Figure 4a, is compared with the standard CPMAS spectrum obtained by processing only the initial FID (Figure 4b). The remarkable enhancement is achieved by using TPPM ^{1}H decoupling, which reduced the width of individual spikelets to less than 0.5 Hz in all silicon sites, allowed to accumulate a series of 200 echoes, and produced a relatively undistorted spectrum.

The sensitivity gain as a function of N for Q^4 and T^3 sites in sample **A** and the fits obtained using eq 1 are shown in Figure 5a. The fitted curves corresponding to all silicon sites in this sample are compared in Figure 5b. The dependence of signal enhancement on T_2 is an obvious shortcoming of the approach utilizing CPMG. Without the aid of ^{1}H decoupling, the T^2 and T^3 resonances would be further attenuated in the CPMG spectra due to more rapid dephasing of their magnetization by the residual dipolar couplings with protons in allyl groups. However, Figure 5b demonstrates that the spectral distortions can be minimized by truncating the CPMG dataset. For example, by reducing the number of echoes to 30, the relative intensities in the reconstructed spectrum of sample **A** are within a few percent

(36) Detken, A.; Hardy, E. H.; Ernst, M.; Meier, B. H. *Chem. Phys. Lett.* **2002**, *356*, 298−304.
(37) Ernst, M.; Samoson, A.; Meier, B. H. *J. Magn. Reson.* **2003**, *163*, 332−339.
(38) Ostroff, E. D.; Waugh, J. S. *Phys. Rev. Lett.* **1966**, *16*, 1097−1098.
(39) Garroway, A. N. *J. Magn. Reson.* **1977**, *28*, 365−371.
(40) Cheng, J. T.; Ellis, P. D. *J. Phys. Chem.* **1989**, *93*, 2549−2555.
(41) Larsen, F. H.; Farnan, I. *Chem. Phys. Lett.* **2002**, *357*, 403−408.
(42) Larsen, F. H.; Jakobsen, H. J.; Ellis, P. D.; Nielsen, N. C. *Mol. Phys.* **1998**, *95*, 1185−1195.
(43) Vosegaard, T.; Larsen, F. H.; Jakobsen, H. J.; Ellis, P. D.; Nielsen, N. C. *J. Am. Chem. Soc.* **1997**, *119*, 9055−9056.
(44) Lefort, R.; Wiench, J. W.; Pruski, M.; Amoureux, J. P. *J. Chem. Phys.* **2002**, *116*, 2493−2501.
(45) Hu, J. Z.; Wind, R. A. *J. Magn. Reson.* **2003**, *163*, 149−162.

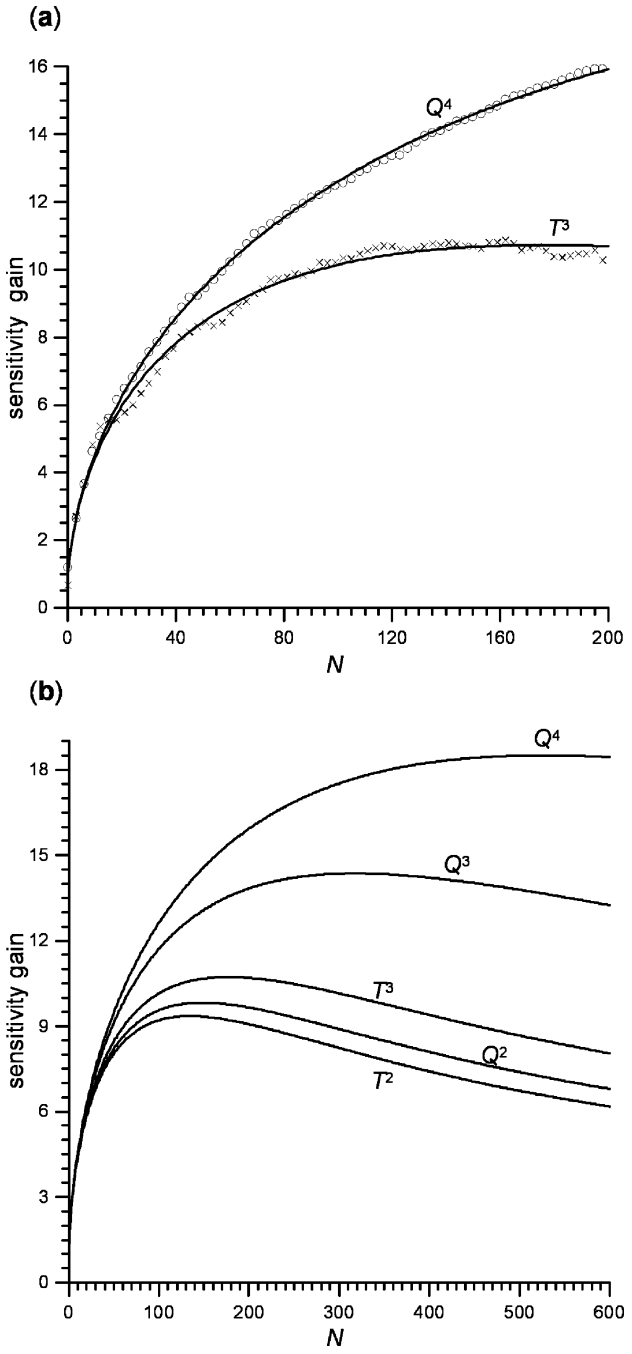

Figure 5. (a) Sensitivity gain as a function of N measured for Q^4 (○) and T^3 (×) sites in sample **A**. Only one out of three data points are shown for $N = 0, 3, 6, \ldots, 198$. The solid lines represent fits obtained using eq 1. (b) Sensitivity gains for all silicon sites in sample **A** obtained by fitting the available experimental points ($0 \le N \le 200$). The curves are extrapolated to $N = 600$.

of those observed in the first FID, while the sensitivity gains are still between 6.8 and 7.5. (Note that for T_2 approaching infinity the gain would be $G(N) = \sqrt{2N+1}$, thus $G(30) = 7.8$.) Similar gains have been observed in several other functionalized MCM-41 samples studied thus far in our laboratory.

The ^{1}H−^{29}Si CPMG-HETCOR spectra of samples **A** and **B** are shown in Figure 6. The pulse sequence applied in this experiment (scheme **3**, Figure 2c) used 200 rotor-synchronized echoes, which were acquired under the same experimental conditions as in the previously discussed 1D CPMAS spectra.

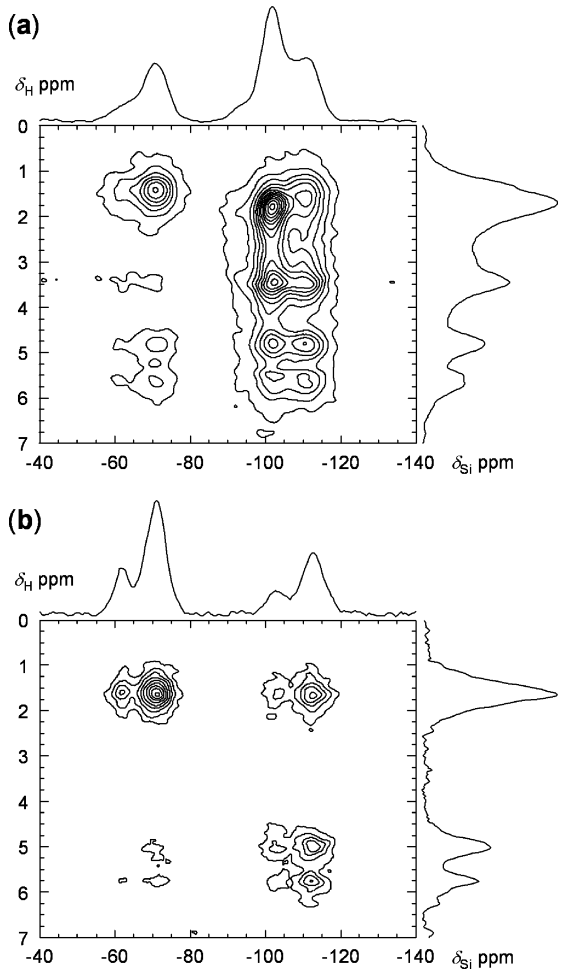

Figure 6. Two-dimensional ^{1}H−^{29}Si CP CPMG-HETCOR spectra of samples **A** (a) and **B** (b) acquired using $\nu_R = 40$ kHz, $\tau_{CPMG} = 5.6$ ms, $N = 200$, $\tau_{CP} = 10$ ms, $\nu_{RF}^{H} = 110-130$ kHz during RAMP-CP, $\nu_{RF}^{H} = 18$ kHz during TPPM decoupling $\nu_{RF}^{Si} = 80$ kHz during CP and π pulses, and a delay between scans of 2.6 s (including 1.1 s of data acquisition). The total acquisition time was 14 h for spectrum (a) and 9 h for spectrum (b). The 1D projections are shown in skyline mode.

The 2D HETCOR spectrum was reconstructed by separating the signals registered before and after each echo maximum, processing the resulting 2D datasets separately, and adding the spectra. Again, we achieved an overall gain in S/N of approximately 1 order of magnitude. Consequently, the ^{1}H−^{29}Si HETCOR spectra of silica surfaces that were essentially "out of reach" under the standard conditions could be easily acquired overnight.

3.4. Interpretation of the Spectra. The ^{1}H−^{13}C spectra of Figure 3 demonstrate that the AL-MCM material was covalently functionalized with the allyl groups as intended. A supplementary measurement of the cross polarization dynamics in sample **A** showed that the CP times were in the order of 300, 450, and 900 μs for C1, C2, and C3 carbons, respectively. These values are several times higher than that expected in fully rigid molecules, which further substantiates the presence of molecular motion. Since the allyl groups are covalently bound to the silica surface, as evidenced by the presence of T^2 and T^3 sites in the ^{29}Si NMR spectra, the mobility must involve rotation around the single C−C bonds.

In the case of sample **B**, the interpretation of ^{1}H−^{29}Si HETCOR spectrum is straightforward because the inorganic

hydrogen atoms on the surface have been eliminated by exchange with deuterium. The strongest cross-peak observed in this sample represents a correlation between silicon site T^3 and H1 hydrogen in the allyl group attached to this site. As expected, the T^2 silicon sites are also correlated with H1 hydrogen. A resonance involving T^2 and the methoxy group (see Figure 3) was not observed, most likely due to high mobility of the $-OCH_3$ group. Also present in Figure 6b are the cross-peaks between H1 and the adjacent Q^3 and Q^4 silicon sites. The cross-peaks between these two silicon sites and hydrogens H2 and H3 are relatively intense, as well. This is a result of spatial proximity rather than $^1H-^1H$ spin diffusion because in the latter case, strong correlations would be also expected between these hydrogens and the T^n sites. Thus, despite having a certain degree of rotational mobility, the $-CH=$ and $=CH_2$ groups strongly interact with the silica surface. It is also noted that all ^1H resonances observed in this spectrum are shifted 0.2−0.3 ppm downfield with respect to sample **A**, due to interaction with D_2O.

All resonances found in sample **B** were also detected in sample **A** (Figure 6a). In addition, cross-peaks are observed between silicon sites and inorganic hydrogen species on the surface, which include rapidly exchanging $\equiv Si-OH\cdots(H_2O)_n$ species and isolated silanol groups. The $\equiv Si-OH\cdots(H_2O)_n$ species, which resonate at around 3.4 ppm, are primarily correlated with the Q^3 and Q^4 sites. A weak correlation between these species and the T^n sites is also observed, indicating that some of the water resides in the vicinity of allyl groups. As expected, the isolated silanol groups show strongest correlations with the Q^3 groups. Note that the resonance due to H1, which dominated the spectrum of sample **B**, is now present as a shoulder of the main peak at 1.8 ppm. The correlations of Q^4 with H1 and Q^4 with the silanols strongly overlap, yielding an unresolved cross-peak centered at around 1.6 ppm.

4. Conclusion

Highly resolved solid-state HETCOR NMR spectra between protons and low gamma nuclei can be conveniently observed on surfaces by using fast MAS. This approach proved very profitable on the functionalized silica surfaces, where MAS at 40 kHz can provide adequate $^1H-^1H$ decoupling. Numerous additional advantages of using fast MAS in HETCOR NMR have been described, which include easy setup, lack of scaling factors, and ease of acquisition of sideband-free spectra. The loss of sensitivity due to small rotor volume ($<10\ \mu L$) is offset by low requirements for the RF field homogeneity within the sample.

In the case of $^1H-^{13}C$ HETCOR NMR, the spectra of surface functional groups on silica can be obtained without using isotope enrichment. In addition, the sensitivity of $^1H-^{29}Si$ HETCOR NMR can be increased very significantly by applying the CPMG train of π pulses to the ^{29}Si spins. The experiments performed thus far indicate that sensitivity gains exceeding 1 order of magnitude are not unusual on the silica surfaces. These experiments require unusually long acquisition periods, which can exceed the duration of the delay between consecutive scans. Under such circumstances, fast MAS offers an additional advantage in that it can be used with low-power heteronuclear decoupling. The applicability of CPMG echoes in $^1H-^{13}C$ HETCOR is not nearly as promising due to more effective T_2 relaxation (especially in case of CH_2 groups) and due to a longer delay τ_{CPMG} which is typically required to avoid truncation of the echoes.

These methods provided detailed characterization of the surface of AL-MCM mesoporous silica. Similar methods are being currently applied in the studies of surfaces functionalized with more complex molecules.[46] Access to smaller surfaces and/or lower molecular concentrations can be gained by using isotopically enriched samples.

Acknowledgment. This research was supported at Ames Laboratory by the U.S. DOE, Office of BES, under Contract W-7405-Eng-82.

JA0509127

(46) Chen, H.-T.; Huh, S.; Wiench, J. W.; Pruski, M.; Lin, V. S.-Y. *J. Am. Chem. Soc.* Submitted.